19 Assessment of Myocardial Blood Volume

Kevin Wei

CONTENTS

19.1 Introduction *277*
19.2 Coronary Microcirculation *277*
19.3 Myocardial Contrast Enhancement and Capillary Blood Volume *278*
19.3.1 Fixed Perfusion Defects *279*
19.3.2 Reversible Perfusion Defects *284*
19.4 Coupling Between Capillary Derecruitment and Hyperemic Flow *288*
19.5 Conclusion *289*
References *289*

19.1 Introduction

Myocardial contrast echocardiography uses microbubbles as a perfusion tracer. The microbubbles approximate the size of red blood cells (2–5 μm), and they remain entirely intravascular; thus, detection of these microbubbles can provide important insights into the integrity of the myocardial microvasculature. Ultrasound has excellent spatial resolution (<1 mm axially), which allows assessment of even transmural differences in myocardial perfusion (Linka et al. 1998; Villanueva et al. 1993). Myocardial contrast echocardiography is therefore ideally suited to evaluate the location, size, and transmural extent of myocardial perfusion defects.

This chapter reviews important aspects of the coronary microcirculation that are pertinent for understanding normal and abnormal myocardial perfusion on contrast echocardiography. The ability of contrast echocardiography to assess spatial aspects of myocardial perfusion (i.e., fixed and reversible perfusion defects), and the pathophysiologic changes that occur in the coronary microcirculation to produce such defects, are discussed. The discussion on perfusion defects focus on applications of contrast echocardiography in the setting of acute myocardial infarction, and on the development of reversible perfusion defects during stress in the setting of coronary artery disease.

K. Wei, MD
Cardiac Imaging Center, Cardiovascular Division, University of Virginia School of Medicine, P.O. Box 800158, Charlottesville, VA 22908-0158, USA

19.2 Coronary Microcirculation

Coronary microcirculation is directly or indirectly involved in a wide array of pathologic states. Its behavior in different diseases and situations can therefore provide important insights into coronary pathophysiology in humans. Having an understanding of microvascular anatomy and characteristics is therefore important for interpreting myocardial contrast echocardiography images.

Detailed descriptions of the coronary systems of many species are now available (Bassingthwaighte et al. 1974; Marcus 1983; Tschabitscher 1984; Anderson et al. 1988; Kassab et al. 1993; Kassab et al. 1994a,b). In particular, studies of the pig heart have provided an understanding of the distribution of blood within the coronary system (Kassab et al. 1993, 1994a,b) and allowed us to appreciate what a myocardial contrast echocardiography image represents.

The arterial and venous systems have branching vessels that can be mathematically characterized as fractals. The venous system has arcading veins in the epicardial and endocardial surfaces in pigs. Arcading arteries are present on the epicardial surface in pigs (Kassab et al. 1993), but they exist on the endocardial surface in humans. The majority of venules drain into the coronary sinus, but some (Thebesian veins) drain directly into the ventricular cavities (Kassab et al. 1994a). For each order of branching, veins in the myocardium are larger than arteries of the same order.

Additionally, myocardial veins are more irregularly shaped than arteries. The myocardial veins are also interconnected, and more than one vein may drain a myocardial region served by a single artery (Kassab et al. 1994a).

Unlike the arterial and venous systems, most capillaries traverse the length of a myocyte, and their orientation is parallel to that of myocardial muscle fibers. The arterioles feeding the capillaries are approximately 10 μm in diameter (the smallest order of branches). Capillaries can also branch directly from up to third-order vessels (the main trunk being eleventh order; Kassab et al. 1994a). Approximately 50% of feeding arterioles run parallel to the capillary bed, and each can give rise to several capillaries.

About 25% of the feeding arterioles course transversely toward the myocyte and give off two capillaries at right angles. The remaining arterioles are a mixture of these two patterns (Kassab et al. 1994a). The draining venules run in the same direction as capillaries before turning obliquely to join higher-order veins. Even though most capillaries drain into first-order venules, they may drain into up to seventh-order venules (the coronary sinus being the thirteenth order) (Kassab et al. 1994b).

Capillaries have been characterized as Y, H, or T depending on their shape. The mean capillary diameter is approximately 6 μm, and the mean length is 0.5–1 mm, depending on the species. The mean intercapillary distance is 15–20 μm (Kassab et al. 1994b; Bassingthwaighte et al. 1974). To provide efficient oxygen delivery, capillaries traverse the length of myocytes, and each capillary has a domain and is responsible for its nutrition. The rate of oxygen diffusion across tissue, and the rate of oxygen consumption by tissue, determine the size of the domain (Gayeski and Honig 1991). The number of capillaries and the intercapillary distance within a tissue depend on the oxygen needs of the specific tissue (Kassab et al. 1994b; Bassingthwaighte et al. 1974). Under resting conditions, not all capillaries allow red blood cell flow. Red blood cell flux is seen in only about half of the capillaries in cardiac muscle (Tillmans et al. 1987). Because myocardial oxygen extraction is already near maximal at rest, adequate oxygen delivery can be met only through increases in myocardial blood flow when myocardial oxygen consumption increases (Le et al. 2002). A mild increase in myocyte oxygen requirements results in a mild increase in red blood cell velocity through capillaries. Further increases in demand, however, require additional mechanisms to increase nutrient delivery. One mechanism for the increase in myocardial O_2 delivery during stress is functional recruitment of capillaries, allowing more red blood cells to pass through more capillaries (Friedman et al. 1995; Le et al. 2002).

The volume of blood within the entire coronary circulation at rest in diastole is approximately 12 ml/100 g of left ventricular myocardium (Kassab et al. 1994a). This volume is distributed almost equally between the arterial (epicardial coronary artery to 200-μm arterioles), microcirculatory (200-μm arterioles to 200-μm venules), and venous compartments (200-μm venules to coronary sinus) – with 3.5, 3.8, and 4.9 ml/100 g in each compartment, respectively. Most of the arterial and venous blood volumes, however, are located on the epicardial surface of the heart. Within the myocardium itself, the capillaries numerically outnumber all other vessels (with a density of 3000–4000/mm^2), and contain almost all the myocardial blood volume. Only 5–10% of myocardial blood volume is contained within intramyocardial arterioles and venules (Kassab et al. 1994a).

19.3 Myocardial Contrast Enhancement and Capillary Blood Volume

The microbubble agents used to evaluate myocardial perfusion during contrast echocardiography are efficient scatterers of US energy. A linear relation exists between low microbubble concentrations and the corresponding backscatter signal displayed on contrast echocardiography, so their relative concentrations in tissue can be quantified (Skyba et al. 1994). The microbubbles are unlike the tracers used with other non-invasive cardiac imaging techniques (such as PET, SPECT, MRI, or CT), because they are hemodynamically inert, and also remain entirely intravascular (Keller et al. 1989).

Relative concentration (or regional video intensity on myocardial contrast echocardiography) of microbubbles in different areas of the myocardium therefore reflect the blood volume in those regions (Linka et al. 1998; Wei et al. 1998a).

Since the largest proportion of myocardial blood volume is contained within capillaries, regional video intensity reflects capillary blood volume; thus, provided that the relation between signal amplitude and tracer concentration is linear, changes in myocardial blood volume are reflected by proportional changes in video intensity on contrast echocardiography (Fig. 19.1) expressing as perfusion defects.

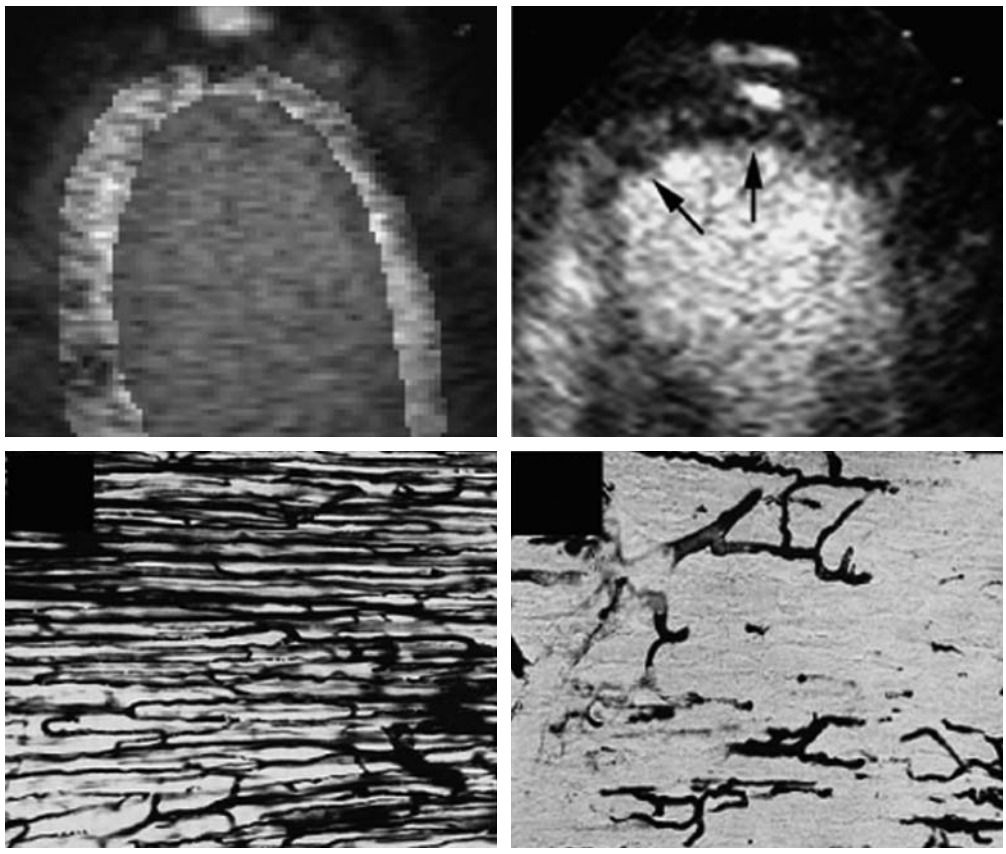

Fig. 19.1a–d. Contrast-enhanced apical three-chamber view shows homogeneous myocardial opacification in all perfusion territories (**a**) representing normal capillary integrity (**c**). A focal subendocardial perfusion defect in patient with prior apical infarction (**b**) is seen (*arrows*) in the presence of capillary damage (**d**).

19.3.1 Fixed Perfusion Defects

The fixed myocardial perfusion defects are those which are evident both during resting and during physical or pharmacologic stress.

a) Application of contrast echocardiography in acute myocardial infarction. Experimental studies in dogs have shown that the time course of cell death begins approximately 30–40 min after acute coronary occlusion (Reimer and Jennings 1979). Necrosis extends from the subendocardium where ischemia is the most severe, towards the subepicardium, and becomes transmural after 6 h. Reperfusion within 2 h can result in functional recovery of the ischemic tissue; thus, early reperfusion of the infarct-related artery has been shown to salvage viable myocardium within the infarct bed. Zones of severe myocellular injury or death are associated with microvascular damage or plugging. Microbubbles will therefore be excluded from these areas, which will manifest as perfusion defects on myocardial contrast echocardiography.

Apart from the duration of occlusion, determinants of infarct size include the size of the risk area, as well as the adequacy of collateral flow (Kaul et al. 1987; Levin 1974; Piek and Becker 1988).

With the advent of contrast echocardiography, there is now a non-invasive method that can assess both of these latter parameters rapidly at the patient's bedside. Furthermore, contrast echocardiography can be used to determine the success of reperfusion. Since the microbubbles have only a short half-life in the circulation, contrast echocardiography can also be used serially to study the effects of interventions in patients with acute myocardial infarction. With its portability and excellent spatial resolution (<1 mm axially), contrast echocardiography may be very useful if incorporated into the assessment of patients with acute myocardial infarction.

b) Detection of Risk Area. The region of myocardium subtended by an occluded coronary artery that may eventually develop necrosis is termed the risk area (Kaul et al. 1984). On myocardial contrast echocardiography, the risk area is a well demarcated zone of hypoperfusion adjacent to neighboring areas of normal myocardial blood flow. After a direct intracoronary injection of microbubbles, the risk area appears as a non-enhanced region of myocardium with a distinct border. In animal models, direct intracoronary (Kaul et al. 1985, 1986), aortic root (Firschke et al. 1997a), right or left atrial (Villanueva et al. 1993; Firschke et al. 1997a), and most recently intravenous (Grayburn et al. 1995; Firschke et al. 1997b; Lindner et al. 1998) injections of microbubbles have all been shown to successfully define the risk area with excellent concordance (Lindner et al. 1998) to intracoronary injections of color dyes or technetium autoradiography (Fig. 19.2).

In acute animal models, it has been shown that the size of the risk area matches closely with the extent of abnormal wall motion on echocardiography (Kaul et al. 1984, 1986). In patients, however, preexisting wall motion abnormalities may be present from prior infarction, acute or chronic ischemia, or cardiomyopathic causes. Evaluation of wall motion alone may not be adequate for the assessment of risk area in many patients, and an assessment of perfusion may provide useful adjunctive information.

Defining the spatial extent of the area at risk may help to guide therapy in the future. For example, patients with a small risk area who have relative contraindications to thrombolytic therapy may have an unacceptable risk of bleeding compared with the benefit of modest myocardial salvage from reperfusion. On the other hand, a large perfusion defect may help to define patients who would derive the greatest benefit from urgent primary angioplasty. It is also possible that the evaluation of perfusion defect size and severity with contrast echocardiography may help identify patients with non-ST ECG trace elevation myocardial infarction who have greater clot burden and may benefit from early institution of potent antiplatelet agents, thrombolytics, or angioplasty. These issues await further clinical studies to demonstrate clinical efficacy.

c) Assessment of the Success of Reperfusion and Determination of Infarct Size. Both morbidity and mortality from myocardial infarction are significantly affected by infarct size, which can be characterized by the endocardial length and/or the transmural extent of the perfusion defect on contrast echocardiography.

Early reperfusion remains the mainstay of therapy for patients presenting with acute myocardial infarction. Clinical markers, including resolution of ST, segment of ECG elevation, alleviation of angina, and ventricular arrhythmias, such as an accelerated idioventricular rhythm, are indicative of tissue reperfusion, but are neither sensitive nor specific (Califf et al. 1988). Wall thickening on echocardiography cannot reliably determine the success of reperfusion either, due to the development of stunning from prolonged ischemia.

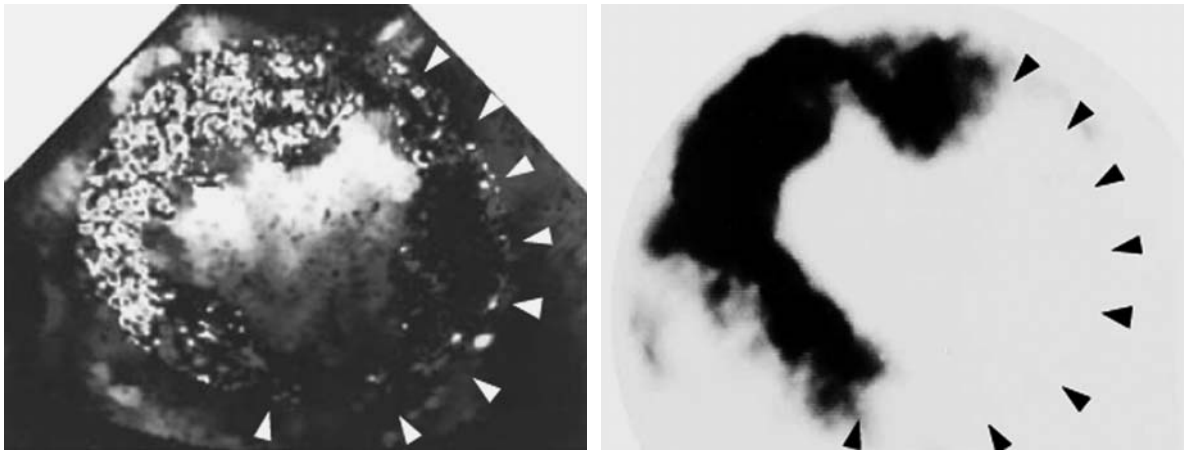

Fig. 19.2a,b. A color-coded short-axis image of the left ventricle after a peripheral intravenous injection of microbubbles in a dog with an occlusion of the left circumflex coronary artery (**a**). A technetium autoradiograph obtained from the same short-axis level is also shown (**b**). The lateral wall (*arrows*) has a well-defined area without contrast enhancement which is clearly separated from the normal bed. The spatial location and extent of the risk area on myocardial contrast echocardiography closely approximates the "cold spot" on the technetium autoradiograph.

A non-invasive perfusion method that can easily and rapidly define the re-establishment of tissue flow would therefore be useful. Apart from assessing the success of therapy, determining those patients with unsuccessful thrombolysis may be beneficial, as they may require further interventions such as rescue angioplasty (Belenkie et al. 1992; Ellis et al. 1994). Myocardial contrast echocardiography therefore has the potential to provide important adjunctive information that may impact the management of patients presenting with acute myocardial infarction.

Even in patients who undergo primary angioplasty, it is now recognized that simple recanalization of the infarct-related artery is inadequate to ensure a good outcome. Perfusion must also be restored at a microvascular level; thus, after blood flow is restored to an occluded bed, myocardial opacification should be seen within regions with successful reperfusion on myocardial contrast echocardiography. Despite patency of the infarct-related artery, myocardial contrast echocardiography can define regions with significant myocellular injury (necrosis) and microvascular disruption, since they show no opacification – or no reflow. This phenomenon may be due to reduced microvascular flow from small vessel spasm or microvessels could be plugged by thrombi, inflammatory cells, or debris.

Due to the excellent spatial resolution of US, the spatial extent and location of even subendocardial infarction can be defined on myocardial contrast echocardiography (Fig. 19.1), and has been shown in animal studies to correlate well with 2,3,5-triphenyltetrazolium chloride assessments of infarct size (Firschke et al. 1997b; Lindner et al. 1998).

Clinical studies have evaluated the relationship between antegrade epicardial flow using the Thrombolysis in Myocardial Infarction study group grading system, and the adequacy of microvascular perfusion on contrast echocardiography. A number of landmark studies have shown that patients with Thrombolysis in Myocardial Infarction grades 1 and 2 flow have a higher incidence of no-reflow on contrast echocardiography compared with those with Thrombolysis in Myocardial Infarction grade 3 flow (Ito et al. 1996a; Iwakura et al. 1996). Even in patients with Thrombolysis in Myocardial Infarction grade 3 flow, however, 16% had microvascular no-reflow on contrast echocardiography (Ito et al. 1996a), and other studies have found even higher incidences (Porter et al. 1998).

The extent of no-reflow on contrast echocardiography has been shown to have significant consequences. Patients with low- or no-reflow had poor recovery of left ventricular function, greater infarct expansion, remodeling, and left ventricular dilation (Ito et al. 1996b; Porter et al. 1998). Moreover, patients with poor microvascular reperfusion have a significantly higher incidence of cardiac events including cardiac death, non-fatal myocardial infarction, and congestive heart failure over a 1-year follow-up period (Sakuma et al. 1998).

More recent studies done with intravenously administered contrast agents show good concordance between contrast echocardiography and SPECT for detection of viability (Fig. 19.2). Dysfunctional segments that demonstrated contrast enhancement had better recovery of wall motion than segments with no-reflow (Rocchi et al. 2001). The presence of reflow defined by myocardial contrast echocardiography 24 h after reperfusion has been found to be associated with higher coronary flow reserve than patients with no-reflow, and these authors also found that these segments had better improvement in regional and global ventricular function at follow-up (Lepper et al. 2000).

d) Evaluation of Collateral Flow in Acute Myocardial Infarction with Contrast Echocardiography. Defining infarct size by assessment of the no-reflow zone is performed only after reperfusion (Dittrich et al. 1995). As mentioned above, the adequacy of collateral flow to the occluded bed influences the extent of necrosis and ultimate infarct size (Maruoka et al. 1986; Sabia et al. 1992); thus, for any given size of risk area and duration of coronary occlusion, the magnitude and extent of collateral flow into the risk area will determine the degree of necrosis and ultimate infarct size.

Prior to the development of new-generation microbubble agents, the ability of direct intracoronary injections of microbubbles to define the presence of collateral flow in patients with recent acute myocardial infarction was shown (Maruoka et al. 1986; Sabia et al. 1992). Even though collaterals may not be present de novo in normal subjects, patients with chronic coronary artery disease have been shown to develop abundant collaterals to ischemic territories (Sabia et al. 1992). Even with persistent coronary occlusion and prolonged absence of antegrade flow, adequate levels of collateral-derived blood flow can allow maintenance of myocardial viability and spares tissue from necrosis (Sabia et al. 1992).

More recently, Coggins et al. (2001) demonstrated that collateral flow can be assessed using intravenously administered microbubbles. The method is

based on providing enough time for microbubble replenishment into the risk area after their destruction, so that slow collateral-derived flow (Coggins et al. 2001) can be imaged (Fig. 19.3). Not only does the presence of contrast enhancement within the risk area define the presence of collateral flow, but myocardial opacification is only seen when myocardial blood flow exceeds approximately 20% of normal resting levels. Since myocytes may remain viable at levels of 25% of normal resting myocardial blood flow (Maruoka et al. 1986; Coggins et al. 2001), the spatial distribution of perfusion within the risk area identifies tissue that may be spared from necrosis despite persistent coronary occlusion; thus, despite a prolonged 6-h occlusion in the animal shown in Fig. 19.3, no infarction developed. Figure 19.3 illustrates how collateral flow can prevent myocellular necrosis and can modulate infarct size despite prolonged occlusion of the epicardial coronary artery. In the same study, the circumferential extent of abnormal wall thickening was found to correlate well with the size of the initial risk area on myocardial contrast echocardiography, but overestimated the eventual infarct size (Coggins et al. 2001). This finding confirmed those of previous studies (Villanueva et al. 1993).

Thus, despite adequate collateral flow to maintain viability, it is insufficient to preserve normal wall

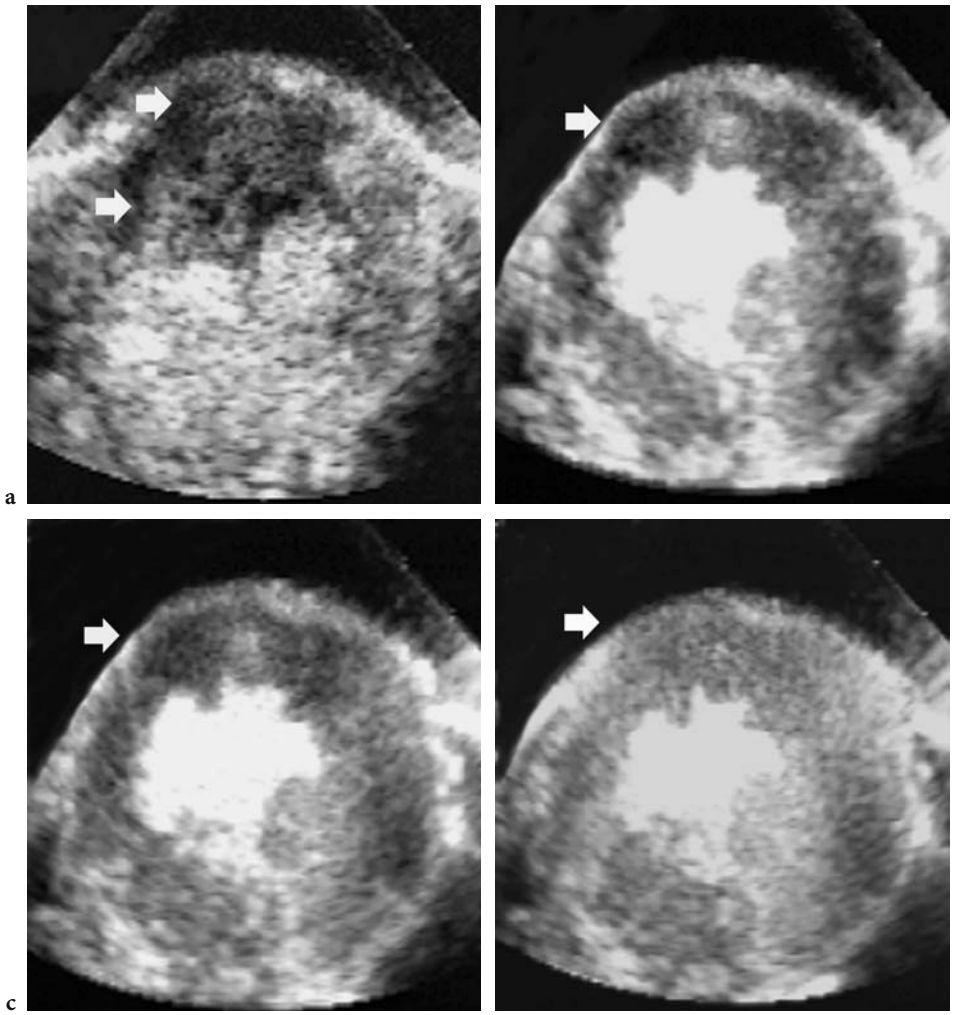

Fig. 19.3a–d. Short-axis images obtained in the presence of an occlusion of the left anterior descending coronary artery, during a continuous intravenous infusion of microbubbles. At the shortest pulsing interval (**a**), a clear demarcation is noted between the inferoposterior wall which has normal myocardial perfusion and the occluded anterior bed, which shows no contrast enhancement (*arrows*). The hypoperfused zone at this pulsing interval represents the risk area. At a longer pulsing intervals of 1.5 and 2.5 s, border zones of the anterior myocardium supplied by collateral flow has started to replenish with microbubbles (**b,c**). At an interval of 10 s, the entire risk area has become homogeneously opacified from collateral-derived myocardial blood flow (**d**). (From Coggins et al. 2001)

thickening. Again, assessments of wall thickening alone therefore provide only limited information in patients presenting with acute myocardial infarction. It cannot be used to predict eventual infarct size, as wall thickening remains severely abnormal even in the presence of adequate collateral flow.

Because the spatial distribution of regions with adequate collateral flow to maintain viability despite persistent coronary occlusion can be defined with myocardial contrast echocardiography, this method can potentially predict infarct size even prior to reperfusion, by defining areas that will be destined to necrose unless reperfusion is achieved (Coggins et al. 2001). As a corollary to the example shown in Fig. 19.3, the short-axis images displayed in Fig. 19.4 demonstrate an animal with a left circumflex coronary occlusion with minimal collateral flow.

Myocardial contrast echocardiography can therefore provide significant information in patients presenting with acute myocardial infarction. It can be used to define the location and spatial extent of the risk area, to evaluate the degree of collateral flow within the risk area, and therefore it can be used to predict eventual infarct size by determining which areas within the risk area will be protected from necrosis by adequate levels of collateral-derived nutrient perfusion. Myocardial contrast echocardiography can also be used serially to evaluate the success of reperfusion therapy, and the assessment of eventual infarct size can provide prognostic infor-

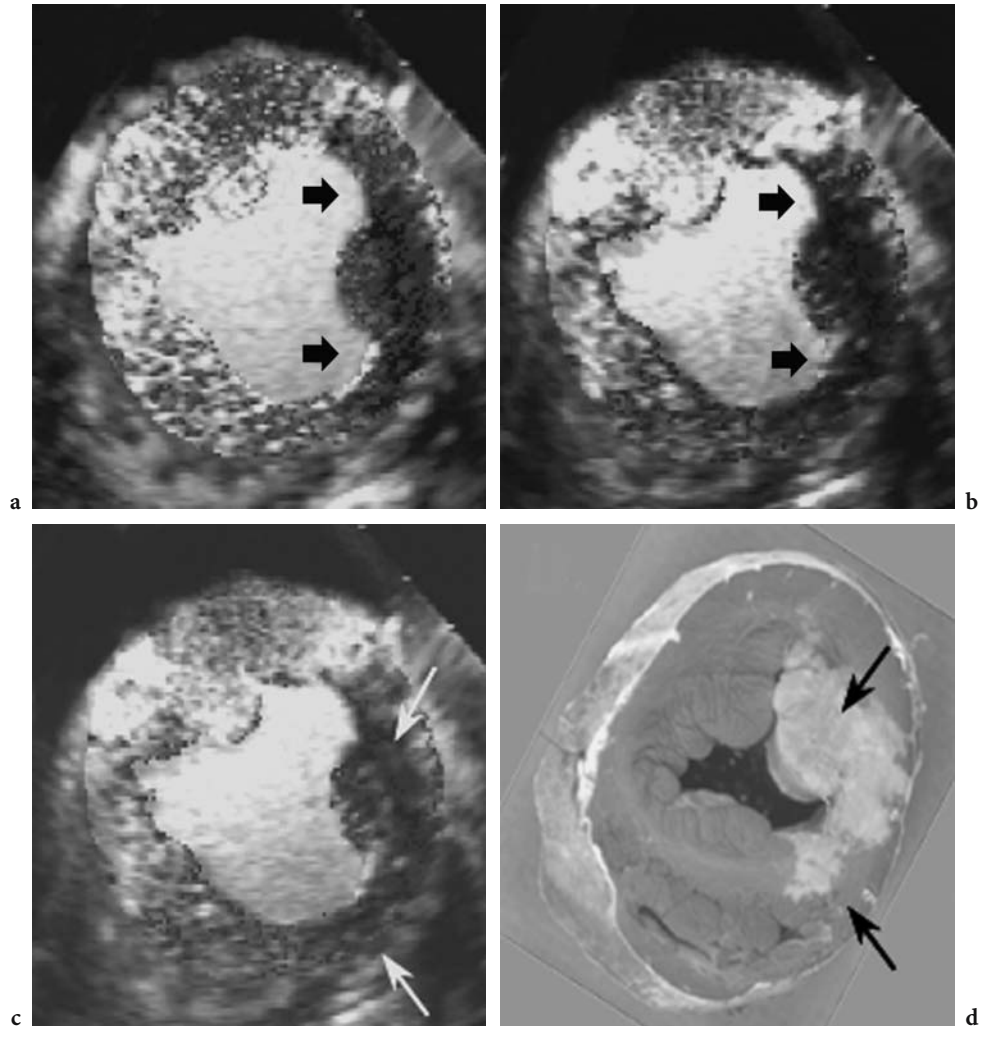

Fig. 19.4a–d. Absence of collateral flow in the risk area during left circumflex occlusion (**a–c**) and subsequent transmural lateral wall infarction (**d**). The risk area in the lateral wall is again seen as a distinct zone of hypoperfusion (*arrows*) at the shortest pulsing interval (**a**). Despite progressive prolongation of the pulsing interval up to 9 s, however, no significant replenishment of microbubbles (*arrows*) is noted within the risk area (**b–c**). After 6 h of occlusion, this animal developed a transmural infarct in the lateral wall demonstrated by the absence of triphenyl tetrazolium chloride staining (*arrows*; **d**). (From Coggins et al. 2001)

mation; however, the exact role of contrast echocardiography in acute myocardial infarction remains to be determined in clinical trials.

19.3.2 Reversible Perfusion Defects

The reversible myocardial perfusion defects are those which become evident during physical or pharmacologic stress and disappear during resting. In the absence of prior myocardial injury, both resting coronary blood flow (Table 19.1) and left ventricular function remain normal even in the presence of an epicardial coronary stenosis up to 85–90% in severity (Fig. 19.5; Gould and Lipscomb 1974). This ability of the myocardium to maintain normal resting myocardial blood flow (Table 19.1) is due to autoregulation, a mechanism by which increases in resistance in one part of the circulation (stenosis in the epicardial coronary artery) are counterbalanced by decreases in another (resistance arterioles; Table 19.1). A histogram representing the distribution of resistances across the normal coronary circulation at baseline is illustrated in Fig. 19.6 (Chilian et al. 1986; Johnson 1986; Jayaweera et al. 1999). This process of autoregulation is operative until a stenosis exceeds approximately 85% in severity, when arteriolar vasodilatory reserve is exhausted. After this point, further decreases in coronary driving pressure will result in decreases in resting coronary blood flow. Since neither coronary blood flow, myocardial blood flow, nor wall motion abnormalities are evident before this, non-critical stenoses cannot be detected at rest using non-invasive perfusion imaging techniques or assessments of resting left ventricular function.

In order to meet increases in myocardial oxygen demand induced by exercise or other forms of stress, coronary blood flow can usually increase four to five times that of resting levels. Coronary arteries with stenoses that encroach more than 50% of the luminal diameter, however, show an attenuated hyperemic response (Fig. 19.5). To detect non-flow limiting stenoses with echocardiography, therefore, adequate exercise or pharmacologic stress is used

Table 19.1 Fundamental formulas of myocardial perfusion.

MBF=Velocity of MBF × MBV
P=CBF × R (=autoregulation formula)

MBF myocardial blood flow, *MBV* myocardial blood volume, *CBF* coronary blood flow, *P* coronary driving pressure, *R* resistance of coronary circulation

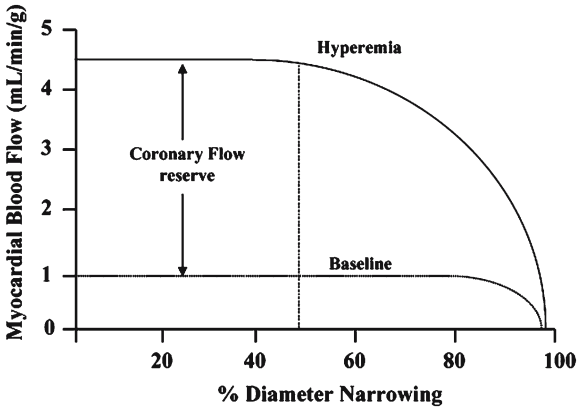

Fig. 19.5 Relation between percentage of stenosis severity and myocardial blood flow at rest and during hyperemia. See text for details. (Redrawn from Gould and Lipscomb 1974)

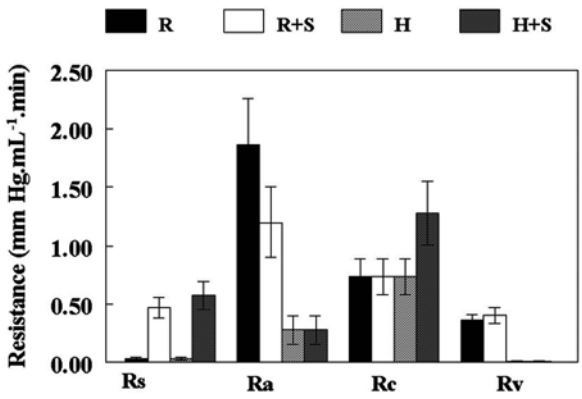

Fig. 19.6 Resistances across the stenosis (*Rs*), arterioles (*Ra*), capillaries (*Rc*), and venules (*Rv*) are shown at rest (*R*), during non-critical stenosis (*R+S*), and during hyperemia in the absence (*H*) and presence of non-critical stenosis (*H+S*). At rest in the absence of stenosis (*R*), the mean aortic pressure of approximately 90 mmHg is reduced to a pre-capillary pressure of 45 mmHg because of arteriolar resistance (R_a), which is the site of greatest resistance to coronary blood flow at rest. There is a further 30 mmHg drop of pressure across the capillary bed. The capillaries are very small in size and offer high resistance, but since they are arranged in parallel, the total capillary resistance decreases with increasing numbers of capillaries (R_c). The drop across the venous bed is only 15 mmHg since these are high-capacitance vessels, which nevertheless have some smooth muscle. Thus, at rest approximately 60% of total myocardial vascular resistance is offered by the arterioles, 25% by the capillaries, and 15% by the venules (R_v). In the presence of a non-critical coronary stenosis (*R+S*), transstenotic resistance (R_s) increases, which results in a decrease in the distal coronary pressure as well as the coronary driving pressure. In this situation, arteriolar vasodilation occurs to decrease arteriolar tone and resistance (R_a). The decrease in arteriolar resistance balances the increase in trans-stenotic resistance, allowing blood flow, pre-capillary arteriolar pressure, and capillary hydrostatic pressure to be maintained at normal resting levels.

to produce supply/demand mismatch and ischemia, which results in the development of a regional wall motion abnormality.

With the advent of perfusion imaging during contrast echocardiography, regional differences in myocardial video intensity between beds with and without stenosis during hyperemia have also been found using intra-arterial, right and left atrial, as well as intravenous bolus injections of microbubbles (Ismail et al. 1995; Firschke et al. 1997b; Wei et al. 1998b). It has been shown in animal models that the severity of reversible perfusion defects that develop on contrast echocardiography correlate with myocardial blood flow mismatch between the normal and stenosed beds determined using radiolabeled microspheres, and that the spatial extent of myocardial contrast echocardiography perfusion defects corresponds to the region showing hypoperfusion by radiolabeled microspheres.

Background-subtracted color-coded images from an animal experiment obtained during hyperemia at baseline and in the presence of left anterior descending coronary artery stenoses of varying severity are shown in Fig. 19.7 which shows the difference between reversible (low-grade coronary stenosis) and fixed (high-grade coronary stenosis) perfusion defects. A good correlation was found between the myocardial video-intensity ratio between the stenosed and normal beds and the degree of myocardial blood flow mismatch between those beds (Wei et al. 1998b).

Similarly, clinical studies performed using bolus injections of microbubbles have shown that abnormal perfusion at rest and during dipyridamole stress can be defined using contrast echocardiography (Kaul et al. 1997; Porter et al. 1997; Heinle et al. 2000). The location of the perfusion defects, and their physiologic relevance (fixed or reversible) are similar to those obtained with ^{99m}Tc-sestamibi SPECT (Kaul et al. 1997; Heinle et al. 2000). Excellent concordance was found when analyses were performed on a segment-by-segment (92%, κ=0.99), territory-by-territory (90%, κ=0.77), or patient-by-patient basis (86%, κ=0.71; Kaul et al. 1997).

a) Mechanism Underlying the Development of Reversible Perfusion Defects on Myocardial Contrast Echocardiography. As with all perfusion defects on myocardial contrast echocardiography, the presence of a reversible perfusion defect denotes the development of relative differences in myocardial blood volume between the stenosed and normal beds after stress that reverses at rest. With bolus injections of microbubbles, however, it was not possible to determine whether the defect was due to an absolute decrease in myocardial blood volume in the stenosed bed, or to an increase in myocardial blood volume in the normal bed during stress (Wei et al. 1998b).

We now know using continuous infusions of microbubbles that capillary derecruitment (or an absolute decrease in myocardial blood volume)

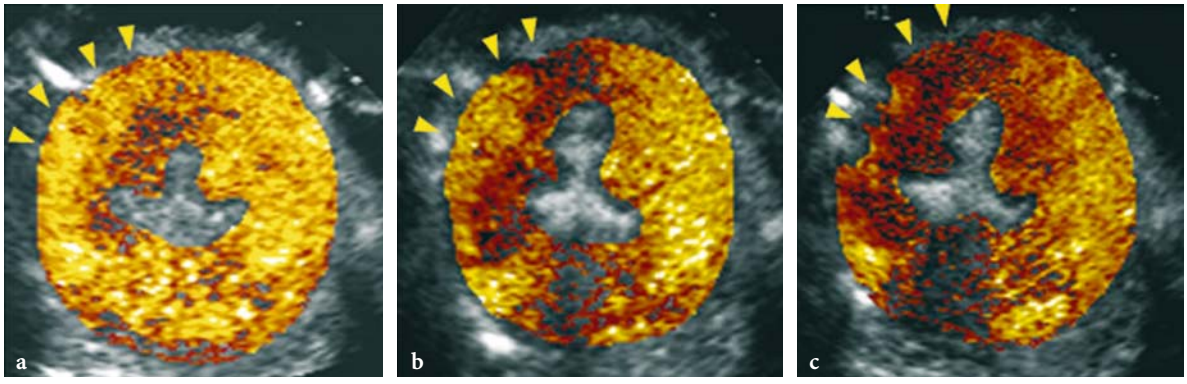

Fig. 19.7a–c. Contrast-enhanced images during hyperemia before (**a**) and in the presence of a mild (**b**) and moderate (**c**) left anterior descending coronary artery stenosis. High concentrations of microbubbles in the left ventricular cavity due to bolus injections produces some attenuation of far-field structures in all the images. Before stenosis placement (**a**), myocardial video intensity is similar between the left anterior descending (*arrows*; 8 to 1 o'clock) and circumflex coronary artery (1 to 5 o'clock) beds. After placement (**b**) of a mild stenosis (trans-stenotic pressure gradient of 14 mmHg), the color in the left anterior descending coronary artery bed takes on more hues of orange and red, denoting a lower myocardial blood volume in the left anterior descending coronary artery (*arrows*) compared with the left circumflex coronary artery bed. Further capillary derecruitment (**c**) develops in the presence of a moderate stenosis (trans-stenotic pressure gradient of 22 mmHg) during hyperemia, causing myocardial video intensity in the left anterior descending coronary artery (*arrows*) bed to also decrease further.

develops in the stenosed bed during stress. We have confirmed that myocardial blood volume decreases in the presence of a stenosis during hyperemia by measuring the myocardial vascular resistance (Fig. 19.8; Wei 2001). We believe that capillaries derecruit distal to a stenosis during hyperemia in order to maintain capillary hydrostatic pressure.

This hypothesis was tested in a model of the coronary circulation consisting of a series of resistances representing the arterial, capillary, and venous beds (Jayaweera et al. 1999). The model assumes that the regulation of coronary blood flow is secondary to changes in resistance of these various compartments, and that the main reason for autoregulation is maintenance of homeostasis and capillary hydrostatic pressure. Using hemodynamic data acquired from animal experiments at four different stages (baseline, maximal hyperemia, epicardial coronary stenosis, and stenosis+hyperemia), resistances from the three circulatory components were derived from the model.

The resistance across the stenosis and the model-derived resistances from the three compartments during the four different experimental settings are shown in Fig. 19.6. When hyperemia was induced in the absence of a stenosis (H), equivalent proportional decreases (approximately 90%) in R_a and R_v developed. The increase in pressure gradient across the capillary bed produces a proportional increase in hyperemic flow, and allows R_c to remain unchanged. During hyperemia (H), however, it is apparent that the compartment with the highest resistance to flow has shifted from the arterioles to the capillaries (Fig. 19.6). When hyperemia was induced in the presence of a non-critical stenosis (H+S), capillary resistance increased further secondary to capillary derecruitment.

Since the length of a capillary does not change, capillary resistance can only increase by reductions of capillary cross-sectional area, or by capillary derecruitment (Jayaweera et al. 1999). The mechanism underlying the derecruitment of capillaries is unclear but occurs in an attempt to maintain capillary hydrostatic pressure (Jayaweera et al. 1999). This mechanism likely prevents unacceptable shifts in fluid distribution between the intra- and extravascular spaces.

Jarhult and Mellander (1973) have previously shown that net transcapillary fluid movement (a measure of capillary hydrostatic pressure) remained essentially constant as skeletal muscle perfusion pressure was varied from 20 to 180 mmHg. Below the lower limit of the autoregulatory range, however, capillary hydrostatic pressure was maintained by increases in postcapillary resistance. It was hypothesized that the increase in venular resistance possibly resulted from passive venular collapse, rheological factors such as increased viscosity at low shear rates, or postcapillary aggregation of red or white blood cells (Jarhult and Mellander 1973). Increases in resistance at the distal end of the capillaries may essentially close the capillary to blood flow.

Investigators have also shown that a severe decrease in perfusion pressure in poststenotic arterioles resulted in capillary derecruitment as determined by an increase in the intercapillary distance visualized by fluorescein-tagged high-molecular dextran (Tillmans and Kuebler 1984). Using

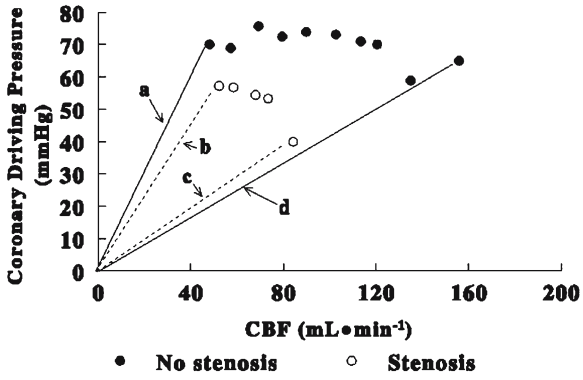

Fig. 19.8 Relation between epicardial coronary blood flow (CBF) and coronary driving pressure (coronary artery pressure–right atrial pressure) derived from an animal in the presence (*open circle*) and absence (*closed circle*) of a non-critical coronary stenosis at rest, and during infusion of adenosine. Myocardial vascular resistance at any level of coronary blood flow and coronary driving pressure is represented by the slope from the origin to that data point. In the absence of a stenosis at rest, coronary driving pressure measured approximately 80 mmHg, with a baseline myocardial blood flow of about 45 ml min^{-1}, and a myocardial vascular resistance denoted by the line *a*. During peak hyperemia, a significant decrease in myocardial vascular resistance (line *d* compared with line *a*) due to arteriolar vasodilation resulted in an almost fourfold increase in coronary blood flow. With placement of a non-flow limiting coronary stenosis, coronary blood flow remains unchanged at 45 ml min^{-1}, but the pressure gradient across the stenosis decreases distal coronary pressure, resulting in a decrease in coronary driving pressure. Resting coronary blood flow remains constant due to a decrease in myocardial vascular resistance (line *b* compared with line *a*), which results from arteriolar vasodilation secondary to autoregulation. When maximal hyperemia is induced in the presence of a stenosis, however, myocardial vascular resistance is higher than expected (line *c* compared with line *d*). Maximal arteriolar vasodilation would have been expected to reduce the myocardial vascular resistance again to line d, but instead, capillary derecruitment that occurs distal to the stenosis during hyperemia increases the myocardial vascular resistance. (From Wei 2001–)

direct intravital microscopy, Tillmans et al. (1991) also showed that in the setting of critical arterial stenosis, capillary and venular diameters did not change significantly, but the ratio of capillaries containing red cells to those containing plasma alone was significantly reduced, producing a functional derecruitment of capillaries.

The decrease in myocardial blood volume that occurs distal to a stenosis during hyperemia underlies the development of reversible perfusion defects not only on contrast echocardiography, but also with other tracers, such as ^{99m}Tc sestamibi. It is currently believed that flow mismatch which develops between the stenosed and normal myocardial beds during hyperemia is the cause of reversible perfusion defects on ^{99m}Tc sestamibi images (Beller and Watson 1991). For flow mismatch to produce a reversible perfusion defect, the uptake of a tracer must be proportional to flow. Relative Tc sestamibi uptake between the hyperemic and control beds, however, remains fairly constant over a wide range of hyperemic flows (Glover and Okada 1990; Glover et al. 1995).

We have recently evaluated the relation between Tc-uptake, regional myocardial blood flow, and myocardial blood volume (Wei et al. 2001). In the first group of dogs, myocardial blood flow was selectively increased in the left anterior descending coronary artery bed with intracoronary infusions of adenosine. During adenosine infusion, mean myocardial blood flow (from all animals) in the left anterior descending coronary artery bed was increased almost three times, while myocardial blood flow in the left circumflex coronary artery bed remained unchanged. Myocardial blood volume between the hyperemic and control beds remained unchanged despite the large regional disparity in myocardial blood flow. Figure 19.9 shows an example of a color-coded parametric image representing myocardial blood volume from a dog where the myocardial blood flow of the left anterior descending coronary artery bed was selectively increased approximately four times that of the control left circumflex coronary artery bed during intracoronary infusion of adenosine; thus, in the absence of changes in capillary blood volume, Tc uptake remains equal despite the presence of significant flow disparity between myocardial beds (Wei et al. 2001). In a second group of dogs, hyperemic flow was induced in both the left anterior descending and the left circumflex coronary artery beds with left main infusions of adenosine. While myocardial blood flow was increased, myocardial blood volume was decreased to different degrees with non-flow-limiting stenoses of different severities in only the left anterior descending coronary artery bed (Fig. 19.10).

These studies indicate that uptake of Tc sestamibi is not dependent on changes in myocardial blood flow, but rather on changes in myocardial blood volume. In the presence of a coronary stenosis during hyperemia, there is capillary derecruitment in the bed distal to a stenosis, which results in a lower capillary surface area for uptake of Tc sestamibi. Decreases in myocardial blood volume, therefore, form the basis for reversible perfusion defects seen on both myocardial contrast echocardiography and Tc sestamibi radionuclide imaging (Wei et al. 2001).

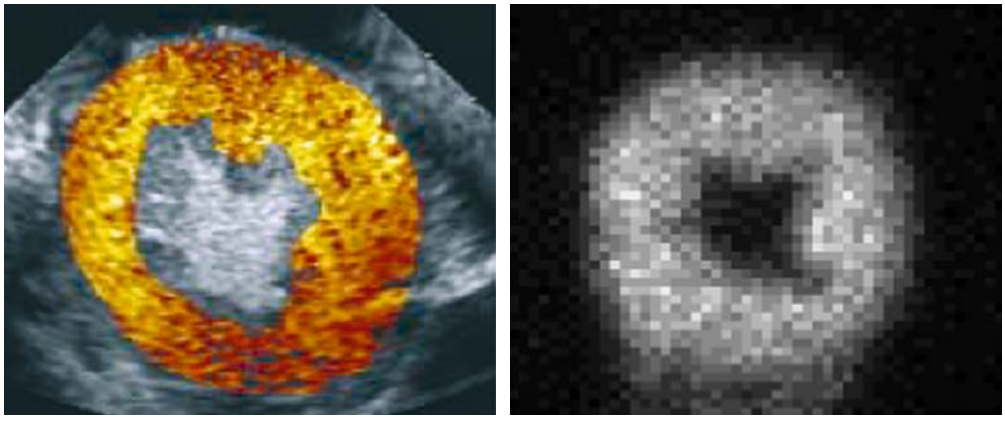

Fig. 19.9a,b. Background-subtracted color-coded contrast echocardiography image (**a**) and corresponding ex vivo Tc-sestamibi image (**b**) obtained during selective left anterior descending hyperemia (10 to 1 o'clock). Despite the large disparity in regional flow between myocardial beds, the entire myocardium shows homogeneous contrast enhancement indicating a similar capillary blood volume in both beds. The corresponding ex vivo Tc-sestamibi image of the same short-axis heart slice also shows equal uptake of sestamibi in the entire myocardium. (From Wei et al. 2001)

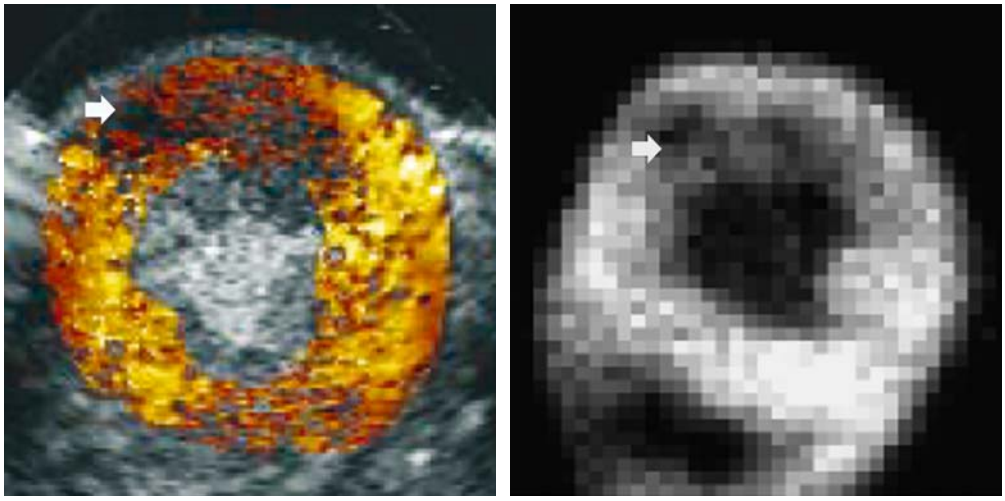

Fig. 19.10a,b. Animal with a moderate left anterior descending coronary artery stenosis. Background-subtracted color-coded contrast echocardiography image (**a**) and corresponding ex vivo Tc-sestamibi image (**b**) obtained during left main infusions of adenosine in the presence of a non-critical left anterior descending stenosis (10 to 1 o'clock). During left main adenosine, myocardial blood flow in the left anterior descending coronary artery bed increased from 1.0 to 2.0 ml min^{-1} g^{-1}. A perfusion defect (*arrow*), indicating a decrease in capillary blood volume, is seen in the left anterior descending coronary artery bed despite the increase in absolute left anterior descending coronary artery flow during hyperemia. The corresponding ex vivo Tc image (**B**) also shows a perfusion defect (*arrow*) that corresponds both in location and spatial extent to the region with decreased capillary blood volume on the myocardial contrast echocardiography image. (From Wei et al. 2001)

b) Summary. A fixed perfusion defect (which means rest and stress perfusion defects) coupled with akinetic wall motion is indicative of myocardial necrosis, while a reversible perfusion defect (stress defect with a normal resting perfusion) coupled with inducible wall motion abnormalities is indicative of myocardial ischemia (Miller and Nanda 2004). In this chapter the myocardial stunning and myocardial hibernation were not mentioned for brevity. Myocardial stunning is defined as a wall motion abnormality in a myocardial territory with a normal perfusion after a recent ischemic insult. Myocardial hibernation is a chronic state of impaired myocardial function at rest, represented by hypokinetic and hypoperfused myocardium, which results from reduced coronary blood flow caused by a critical coronary stenosis and which may be reversed by improving blood flow to the affected myocardium.

19.4 Coupling Between Capillary Derecruitment and Hyperemic Flow

Irrespective of the mechanism producing capillary derecruitment in the presence of a stenosis during hyperemia, the increase in capillary resistance affects hyperemic myocardial blood flow. As discussed, capillaries offer the greatest resistance to hyperemic flow. Increases in capillary resistance therefore reduce hyperemic flow, resulting in a coupling between decreases in capillary blood volume and hyperemic myocardial blood flow and producing reversible perfusion defects. The more severe the stenosis, the greater the degree of capillary derecruitment, the greater the increase in capillary resistance during hyperemia, and the greater the limitation of hyperemic flow.

As shown in the previous and current chapters, myocardial contrast echocardiography has the ability to separately assess both components of myocardial blood flow, namely, velocity of myocardial blood flow as well as myocardial blood volume (Table 19.1). With ^{99m}Tc-sestamibi SPECT, however, only regional decreases in myocardial blood volume are assessed. In the presence of mild or moderate stenoses, subtle differences in myocardial blood volume may not be detectable due to insufficient disparity in counts (<25%) between beds (Glover et al. 1995). On the other hand, contrast echocardiography has far superior spatial resolution (<1 vs 15 mm) and can detect mild subendocardial defects more readily. Furthermore, even if subtle decreases

in myocardial blood volume are not detectable on myocardial contrast echocardiography, regional differences in myocardial blood flow velocity reserve during hyperemia may allow detection of coronary artery disease.

Myocardial contrast echocardiography therefore has features that may allow greater sensitivity for detection of coronary artery disease, and preliminary evidence shows that the combined assessment of myocardial blood flow velocity reserve and myocardial blood volume with myocardial contrast echocardiography may improve detection of mild to moderate coronary artery disease compared with SPECT (Wei et al. 2003).

19.5 Conclusion

Myocardial contrast echocardiogarphy is a versatile technique with excellent spatial and temporal resolution. Perfusion defects on contrast echocardiogarphy, irrespective of whether they are fixed or reversible, are related to relative differences in myocardial blood volume. More importantly, the presence of contrast enhancement on myocardial contrast echocardiogarphy provides an assessment of microvascular integrity, and thus, myocardial viability. Combined with the ability to evaluate red blood cell kinetics, myocardial contrast echocardiogarphy can be used to define the risk area, the adequacy of collateral flow, success of reperfusion, and eventual infarct size in the setting of acute myocardial infarction. These insights may provide new management paradigms for these patients.

Myocardial contrast echocardiogarphy has also provided new insights into the pathophysiologic behavior of the capillary bed in the presence of coronary artery disease during hyperemia, and has allowed us to demonstrate the important role of capillaries in regulating hyperemic flow. Contrast echocardiogarphy has also provided a cohesive relation between changes in myocardial blood volume and myocardial blood flow reserve, and the assessment of either variable can be used to detect and quantify coronary stenosis severity. Because myocardial contrast echocardiogarphy can non-invasively evaluate both specific components of myocardial blood flow, it is a powerful tool that can be used in a broad range of patients with coronary artery disease, extending from the diagnosis of occult stenosis to acute myocardial infarction.

References

Anderson WD, Anderson WB, Seguin RJ (1988) Microvasculature of the bear heart demonstrated by scanning electron microscopy. Acta Anat 131:305–313

Bassingthwaighte JB, Yipintsoi T, Harvey RB (1974) Microvasculature of the dog left ventricular myocardium. Microvasc Res 7:229–249

Belenkie I, Trabousi M, Hall C et al (1992) Rescue angioplasty during myocardial infarction has a beneficial effect on mortality: a tenable hypothesis. Can J Cardiol 8:357–362

Beller GA, Watson DD (1991) Physiological basis of myocardial perfusion imaging with the technetium-99m agents. Semin Nucl Med 21:173–181

Califf RM, O'Neill W, Stacks RS et al (1988) Failure of simple clinical measurements to predict perfusion status after intravenous thrombolysis. Ann Intern Med 108:658–662

Chilian WM, Harrison DG, Haws CW et al (1986) Adrenergic coronary tone during submaximal exercise in the dog is produced by circulating catecolatives. Evidence for adrenergic denervation supersensitity in the myocardium but not in coronary vessels. Circ Res 58(1)68–82

Coggins MP, Sklenar J, Le E et al (2001) Noninvasive prediction of ultimate infarct size at the time of acute coronary occlusion based on the extent and magnitude of collateral-derived myocardial blood flow. Circulation 104:2471–2477

Dittrich HC, Bales GL, Kuvelas T et al (1995) Myocardial contrast echocardiography in experimental coronary artery occlusion with a new intravenously administered contrast agent. J Am Soc Echocardogr 8:465–474

Ellis SG, da Silva ER, Heyndrickx G et al (1994) Randomized comparison of rescue angioplasty with conservative management of patients with early failure of thrombolysis for acute anterior myocardial infarction. Circulation 90:2280–2284

Firschke C, Lindner JR, Goodman NC et al (1997a) Myocardial contrast echocardiography in acute myocardial infarction using aortic root injections of microbubbles in conjunction with harmonic imaging: potential application in the cardiac catheterization laboratory. J Am Coll Cardiol 29:207–216

Firschke C, Lindner JR, Wei K et al (1997b) Myocardial perfusion imaging in the setting of coronary artery stenosis and acute myocardial infarction using venous injection of a second-generation echocardiographic contrast agent. Circulation 96:959–967

Friedman BJ, Grinberg OY, Isaacs KA et al (1995) Myocardial oxygen tension and relative capillary density in isolated perfused rat hearts. J Mol Cell Cardiol 27:2551–2558

Gayeski TE, Honig CR (1991) Intracellular PO2 in individual cardiomyocytes in dogs, cats, rabbits, ferrets, and rats. Am J Physiol 260:H552–H531

Glover DK, Okada RD (1990) Myocardial kinetics of Tc-MIBI in canine myocardium after dipyridamole. Circulation 81:628–637

Glover DK, Ruiz M, Edwards NC et al (1995) Comparison between ^{201}Tl and ^{99m}Tc Sestamibi uptake during adenosine induced vasodilation as a function of coronary stenosis severity. Circulation 91:813–820

Gould KL, Lipscomb K (1974) Effects of coronary stenoses

on coronary flow reserve and resistance. Am J Cardiol 34:48–55

Grayburn PA, Erickson JM, Escobar J et al (1995) Peripheral intravenous myocardial contrast echocardiography using a 2% dodecafluoropentane emulsion: identification of myocardial risk area and infarct size in the canine model of ischemia. J Am Coll Cardiol 26:1340–1347

Heinle SK, Noblin J, Goree–Best P et al (2000) Assessment of myocardial perfusion by harmonic power Doppler imaging at rest and during adenosine stress. Comparison with ^{99m}Tc-sestamibi SPECT imaging. Circulation 102:55–60

Ismail S, Jayaweera AR, Goodman NC et al (1995) Detection of coronary stenosesand quantification of the degree and spatial extent of blood flow mismatch during coronary hyperemia with myocardial contrast echocardiography. Circulation 91:821–830

Ito H, Okamura A, Iwakura K et al (1996a) Myocardial perfusion patterns related to thrombolysis in myocardial infarction perfusion grades after coronary angioplasty in patinets with acute anterior wall myocardial infarction. Circulation 93:1993–1999

Ito H, Maruyama A, Iwakura K (1996b) Clinical implications of the "no reflow" phenomenon. A predictor of complications and left ventricular remodeling in reperfused anterior wall myocardial infarction. Circulation 93:223–228

Iwakura K, Ito H, Takiuchi S et al (1996) Alternation in the coronary blood flow velocity pattern in patients with no reflow and reperfused acute myocardial infarction. Circulation 94:1269–1275

Jarhult J, Mellander S (1973) Autoregulation of capilalry hydrostatic pressure in skeletal muscle during regional arterial hypo- and hypertension. Acta Physiol Scand 91:32–41

Jayaweera AR, Jayaweera AR, Wei K et al (1999) Fate of capillaries distal to a stenosis. Their role in determining coronary blood flow reserve. Am J Physiol 46:H2363–H2372

Johnson Paul C (1986) Autoregulation of blood flow. Circ Res 59:483–495

Kassab GS, Lin DH, Fung YB (1993) Morphometry of pig coronary arterial trees. Am J Physiol 265:H350–H365

Kassab GS, Lin DH, Fung YB (1994a) Morphometry of the pig coronary venous system. Am J Physiol 267:H2100–2113

Kassab GS, Lin DH, Fung YB (1994b) Topology and dimensions of pig coronary capillary network. Am J Physiol 267: H319–H325

Kaul S, Pandian NG, Okada RD et al (1984) Contrast echocardiography in acute myocardial ischemia. I. In vivo determination of total left ventricular "area at risk". J Am Coll Cardiol 4:1272–1282

Kaul S, Gillam L, Weyman AE (1985) Contrast echocardiography in acute myocardial ischemia. II. The effect of site of injection of contrast agent on the estimation of area at risk for necrosis after coronary occlusion. J Am Coll Cardiol 6:825–830

Kaul S, Pandian NG, Gillam LD et al (1986) Contrast echocardiography in acute myocardial ischemia. III. An in-vivo comparison of the extent of abnormal wall motion with the "area at risk" for necrosis. J Am Coll Cardiol 7:383–392

Kaul S, Pandian NG, Guerrero L et al (1987) Effects of selectively altering collateral driving pressure on regional perfusion and function in occluded coronary bed in the dog. Circ Res 61:77–85

Kaul S, Senior R, Dittrich H et al (1997) Detection of coronary artery disease using myocardial contrast echocardiography: comparison with 99mTc sestamibi single photon emission computed tomography. Circulation 96:785–792

Keller MW, Segal SS, Kaul S, Duling B (1989) The behaviour of sonicated albumin microbubbles within the microcirculation: a basis for their use during myocardial contrast echocardiography. Circ Res 65:458–467

Le DE, Bin JP, Coggins MP et al (2002) Relation between myocardial oxygen consumption and myocardial blood volume: a study using myocardial contrast echocardiography. J Am Soc Echocardiogr 15:857–863

Lepper W, Hoffmann R, Kamp O et al (2000) Assessment of myocardial reperfusion by intravenous myocardial contrast echocardiography and coronary flow reserve after primary percutaneous transluminal coronary angiography in patients with acute myocardial infarction. Circulation 101:2368–2374

Levin DC (1974) Pathways and functional significance of the coronary collateral circulation. Circulation 50:831–837

Lindner JR, Firschke C, Wei K et al (1998) Myocardial perfusion characteristics and hemodynamic profile of MRX-115, a venous echocardiographic contrast agent, during acute myocardial infarction. J Am Soc Echocardiogr 11:36–46

Linka AZ, Sklenar J, Wei K et al (1998) Spatial distribution of microbubble velocity and concentration within the myocardium: insights into the transmural distribution of myocardial blood flow and volume. Circulation 98:1912–1920

Marcus ML (1983) Anatomy of the coronary vasculature. In: Marcus ML (ed) The coronary circulation in health and disease. McGraw-ill, New York, pp 3–21

Maruoka Y, Tomoike H, Kawachi Y et al (1986) Relations between collateral flow and tissue salvage in the risk area after acute coronary occlusion in dogs: a topographical analysis. Br J Exp Pathol 67:33–42

Miller AP, Nanda NC (2004) Contrast echocardiography: new agents. Ultrasound Med Biol 30:425–434

Piek J, Becker AE (1988) Collateral blood supply to the myocardium at risk in human myocardial infarction: a quantitative postmortem assessment. J Am Coll Cardiol 11:1290–1296

Porter TR, Li S, Kilzer K, Deligonul U (1997) Effect of significant two-vessel versus one-vessel coronary artery stenosis on myocardial contrast defects observed with intermittent harmonic imaging after intravenous contrast injection during dobutamine stress echocardiography. J Am Coll Cardiol 30:1399–1406

Porter TR, Li S, Oster R, Deligonul U (1998) The clinical implications of no reflow demonstrated with intravenous perfluorocarbon containing microbubbles following restoration of thrombolysis in myocardial infarction (TIMI) 3 flow in patients with acute myocardial infarction. Am J Cardiol 82:1173–1177

Reimer KA, Jennings RB (1979) The "wavefront phenomenon" of myocardial ischemic cell death. II. Transmural progression of necrosis within the framework of ischemic bed size (myocardium at risk) and collateral flow. Lab Invest 40:633–644

Rocchi G, Kasprzak JD, Galema TW et al (2001) Usefulness of power Doppler contrast echocardiography to identify reperfusion after acute myocardial infarction. Am J Cardiol 87:278–282

Sabia PJ, Powers ER, Jayaweera AR et al (1992) Functional significance of collateral blood flow in patients with recent acute myocardial infarction: a study using myocardial contrast echocardiography. Circulation 85:2080–2089

Sakuma T, Hayashi Y, Sumii K et al (1998) Prediction of short- and intermediate-term prognoses of patients with acute myocardial infarction using myocardial contrast echocardiography one day after recanalization. J Am Coll Cardiol 32:890–897

Skyba DM, Jayaweera AR, Goodman NC et al (1994) Quantification of myocardial perfusion with myocardial contrast echocardiography from left atrial injection of contrast: implications for venous injection. Circulation 90:1513–1521

Tillmanns H, Kuebler W (1984) What happens in the microcirculation? In: Hearse DJ, Yellon DM (eds) Approaches to myocardial infarct size limitation. Raven, New York

Tillmans H, Leinberger H, Neumann FJ et al (1987) Myocardial microcirculation in the beating heart: in vivo microscopic studies. In: Spaan JAE, Bruschke AVG, Gittenberger-de Groot AC (eds) Coronary virculation. Nijhoff, Dordrecht, pp 88–94

Tillmanns H, Steinhausen M, Leinberger H et al (1991) Hemodynamics of the coronary microcirculation during myocardial ischemia. Circulation (Suppl) IV:40

Tschabitscher M (1984) Anatomy of coronary veins. In: Mohl W, Wolner E, Glogar D (eds) The coronary sinus: proceedings of the first international symposium on myocardial protection via the coronary sinus. Steinkopff, Darmstadt, pp 8–25

Villanueva FS, Glasheen WP, Sklenar J, Kaul S (1993) Assessment of risk area during coronary occlusion and infarct size after reperfusion with myocardial contrast echocardiography using left and right atrial injections of contrast. Circulation 88:596–604

Wei K, Jayaweera AR, Firoozan S et al (1998a) Quantification of myocardial blood flow using ultrasound-induced destruction of microbubbles administered as a constant venous infusion. Circulation 97:473–483

Wei K, Jayaweera AR, Firoozan S et al (1998b) Basis for detection of stenosis using venous administration of microbubbles during myocardial contrast echocardiography: Bolus or continuous infusion? J Am Coll Cardiol 32:252–260

Wei K (2001) Detection and quantification of coronary stenosis severity with myocardial contrast echocardiography. Prog Cardiovasc Dis 44:81–100

Wei K, Le E, Bin JP, Coggins M et al (2001) Mechanism of reversible ^{99m}Tc-sestamibi perfusion defects during pharmacologically induced coronary vasodilation. Am J Physiol 280:H1896–H1904

Wei K, Crouse L, Weiss J et al (2003) PB127 phase 2 trial results: detection of coronary disease with rest and dipyridamole stress myocardial contrast echocardiography compared to ^{99m}Tc-sestamibi single photon emission computed tomography. Am J Cardiol 91:1293–1298

Special Topics